Journal of
www. biophotonics-journal.org
BIOPHOTONICS

WILEY-VCH

J. Biophotonics **8**, No. 11–12, 944–951 (2015) / **DOI** 10.1002/jbio.201400136

Journal of BIOPHOTONICS

FULL ARTICLE

Fluorescence life-time imaging and steady state polarization for examining binding of fluorophores to gold nanoparticles

Shmulik Schwartz[1, 2, 3], *Dror Fixler*[2, 3], *Rachela Popovtzer*[2, 3], *and Orit Shefi*[*, 2, 3]

[1] Gonda Multidisciplinary Brain Research Center, Bar Ilan University, 5290002 Ramat Gan, Israel
[2] Faculty of Engineering, Bar Ilan University, 5290002 Ramat Gan, Israel
[3] Institute of Nanotechnology and Advanced Materials, Bar Ilan University, 5290002 Ramat Gan, Israel

Received 13 November 2014, revised 1 January 2015; 29 January 2015, accepted 16 February 2015
Published online 9 March 2015

Key words: nanoparticles, gold nanoparticles, fluorescence polarization, fluorescence life time

Nanocomposites as multifunctional agents are capable of combing imaging and cell biology technologies. The conventional methods used for validation of the conjugation process of nanoparticles (NPs) to fluorescent molecules such as spectroscopy analysis and surface potential measurements, are not sufficient. In this paper we present a new and highly sensitive procedure that uses the combination of (1) fluorescence spectrum, (2) fluorescence life-time, and (3) steady state fluorescence polarization measurements. We characterize and analyze gold NPs with Lucifer yellow (LY) surface coating as a model. We demonstrate the ability to differentiate between LY-GNP (the conjugated complex) and a mixture of coated NP and free dyes. We suggest the approach for neuroscience applications where LY is used for detecting and labeling cells, studying morphology and intracellular communications.

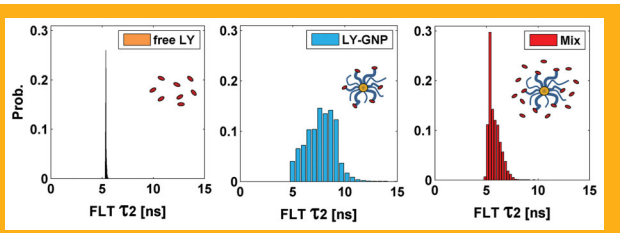

Histograms of Fluorescence lifetime imaging (FLIM) of free LY dye (Left) in comparison to the conjugated dye to gold nanoparticles, LY-GNP (Middle) enable the differentiation between LY-GNP (the conjugated complex) and a mixture of coated NP and free dyes (Right).

1. Introduction

In recent years there has been a dramatic growth in the use of nanoparticles (NPs) in diverse research directions and applications [1, 2]. NPs serve in several biotechnological and biomedical fields, such as imaging [3–9], drug delivery [4, 10], and novel nanodevices [11–14].

The conjugation of fluorescent molecules and NPs is appealing due to their many advantages over fluorescent dyes alone; these nanocomposites have the capability to enhance, quench or re-activate the fluorescent emission [6, 15–17], and to create modifications in fluorescence parameters [6, 18]. In addition, surface modification enables conjugation of different molecules to a single NP for specific targeting [19], increasing cell uptake and biological barrier penetration [20, 21].

Nanocomposites as multifunctional agents are capable of combing imaging and cell biology tech-

* Corresponding author: e-mail: orit.shefi@biu.ac.il, Phone: +972-3-5317079, Fax: +972-3-7384051

nologies. Developing such agents is beneficial for multidisciplinal challenges, for example, in the field of neuroscience for neuropathological diseases, neural regeneration and brain machine interfaces [12, 22, 23]. However, the conventional methods used for validation of the conjugation process (between the NPs and the fluorescent molecule) are not sufficient. Current measurements of surface conjugation are based on spectroscopy analysis, combined with other analytical methods such as size and surface potential measurements. We argue that the conjugation process is better evaluated with a fluorescent based approach.

In this paper we present a new and highly sensitive approach for assessing surface conjugation of NPs with dye probes. We propose to use the combination of procedures including the use of (1) fluorescence spectrum, (2) fluorescence lifetime (FLT) and (3) steady state fluorescence polarization (FP) measurements [24]. Using these methods together provide complementary information on the material characterization and environment [18, 24]. We introduce gold NPs (GNPs) coated with Lucifer yellow (LY) fluorophores as a model for evaluations. GNPs are commonly used agents for a wide range of applications for their simplified synthesis, ease to covalently attach suitable functional organic molecules, stable product, and lack of toxicity [1, 19, 25, 26]. LY is a non-toxic fluorescent dye, widely used in neuroscience for detecting and labeling neurons, for the study of morphology and intracellular communications, both *in vitro* and *in vivo* [27]. The goal of this study is to demonstrate the new fluorescence-based approach as a clear-cut method to determine surface coating and quality of conjugation.

The GNPs were synthesized and their surface was absorbed with PEG to create a protective layer. About 10% of the PEGs were covalently linked to the LY dye. Then, the conjugation to the LY dye was analyzed using FP and FLT imaging (FLIM), in competition to traditional spectrum analysis methods commonly used by manufactures as a quality control for conjugated fluorophores. The fluorescence-based methods demonstrated a better ability to differentiate between coated and uncoated GNPs. Thus, we propose new highly sensitive fluorescence-based procedures for assessing surface conjugation of NPs with dye probes, providing a useful tool for incorporating functional nanocomposites in cells.

2. Materials and methods

2.1 Preparation of particles

Synthesis: 20 nm GNPs were prepared using Sodium Citrate, according to the methodology described by Enüstün and Turkevich [28]. Briefly, 0.414 mL of 1.4 M $HAuCl_4$ solution in 200 mL water was added to a 250 mL single-neck round bottom flask and stirred in an oil bath on a hot plate until boiled. 4.04 mL of a 10% sodium citrate solution (0.39 M sodium citrate tribasic dihydrate 98%, Sigma cas 6132-04-3) was then quickly added. The solution was stirred for 5 min, and then the flask was removed from the hot oil and placed aside until cooled. A small amount of the GNP solution was low speed centrifuged to dispose of excess citrate. This sub-product was termed free GNP.

Conjugation: The surface of the GNPs was absorbed with PEG as a protective layer in order to reduce nonspecific interactions and prevent aggregations. The PEG layer consisted of a mixture of mPEG-SH (thiol-polyethylene-glycol) (~90%, MW ~5000 gr/mol) and a SH-PEG-COOH (heterofunctionalthiol-PEG-acid) (~10%, MW ~5000 gr/mol) (Creative PEGWorks, Winston Salem, NC). The SH-PEG-COOH layer (about 10% of the PEGs) also provided the chemical groups required for fluorophore conjugation (–COOH). First, the solution was centrifuged to dispose of excess citrate. PEG solution was then added to the GNP solution and stirred overnight. This sub-product was termed PEG-GNP. Next, excess EDC (N-ethyl-N -(3-dimethylaminopropyl) carbodiimide) (MW 191.7 gr/mol) and NHS (N-hydroxysuccinimide) (MW 217.13 gr/mol) (Thermo Fisher Scientific, Inc, Rockford, IL) were added to the solution, followed by addition of LY fluorophore molecule (Lucifer yellow CH, lithium salt, MW 457.24 gr/mol, Molecular Probes). NHS and EDC - form an active ester intermediate with the –COOH functional groups, which can then undergo an amidation reaction with the LY $–NH_2$ group. The solution was stirred overnight. This sub-product containing the LY conjugated GNPs and the free LY was termed 'FreeLY-GNP-LY-Mix'. Finally, the solution was placed in a centrifuge in order to dispose the excess of PEG, NHS, EDC and free LY molecules. This sub-product containing the conjugated LY-GNPs was termed LY-GNP. Illustration of the procedure is shown in Figure 1.

Four sub-products of NPs in the synthesis and conjugation process were compared (Figure 1c): (1) GNPs after synthesis and low speed centrifuged (termed 'free GNP'), (2) GNPs with PEG absorbed after high speed centrifuged (termed 'PEG-GNP'), (3) GNPs with PEG and LY coating in a solution excessed with free LY molecules, before centrifuged (termed 'FreeLY-GNP-LY-Mix' or 'Mix' for short), and (4) a solution containing only GNPs with PEG and LY coating after centrifuged without free LY (termed 'LY-GNP'). In addition, these NPs were compared to (5) free LY dye. All samples are in water based solutions.

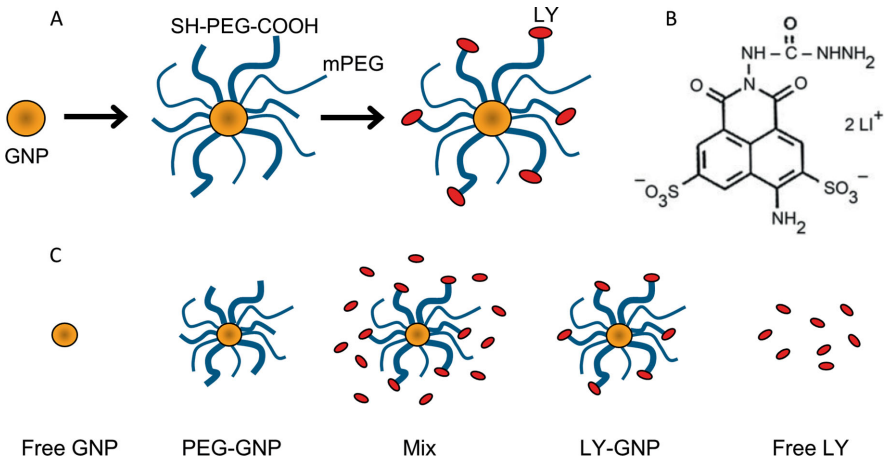

Figure 1 (**A**) Schematic representation of the GNP core (orange) with PEG covering (blue curves) and LY fluorophore (red). (**B**) The molecular structure of Lucifer yellow CH, Li^+ salt [27]. (**C**) The 5 NPs compared in the study are successive steps in the synthesis of LY-GNP. Mix stands for FreeLY-GNP-LY-Mix sample.

2.2 *Particle measurements*

The GNPs were characterized with various methods. Particle size and uniformity were characterized using DLS (Dynamic Light Scattering) for hydrodynamic diameter measurements (ZetaSizer nano ZS, Malvern Instruments, UK). Particle surface coating was analyzed using zeta potential (ZetaSizer nano ZS, Malvern Instruments, UK), and spectrophotometer. In addition, the fluorescence dye conjugation was characterized using measurements for excitation spectra, FP and FLIM.

Spectra analysis used ultraviolet-visible spectroscopy (Carry 100 scan, Agilent Technologies, USA, and UV-1650PC, SHIMADZU, Japan) for absorption, and fluorescence spectrophotometer (Carry eclipse, Agilent Technologies, USA) for excitation. Technical parameters for emission measurements: excitation wavelength 430 nm, excitation slit 5 nm, emission slit 10 nm (5 nm for free LY), PMT voltage 800 mV, and scan rate 30 nm/min. Spectral resolution was ~2 nm.

FP measurements (Carry eclipse, Agilent Technologies, USA) were performed with an excitation wavelength of 430 nm, and 3 repetitions of emission wavelength at 540, 550, and 560 nm, without any significant changes between them. Only data intensity >20 units (arbitrary units- AU) was taken to analysis. Technical parameters for FP measurements: excitation slit of 5 nm, emission slit of 10 nm (5 nm for free LY), PMT voltage 1000 mV (700 mV for free LY), and scan rate 30 nm/min.

The FP experiment is commonly based on the following procedure: monochromatic light passes through a vertical polarizing filter and excites fluorescent molecules in the sample tube. Molecules with the identical vertical polarized plane as the filter can absorb the light, become excited, and subsequently emit light. The emitted light is measured in both the horizontal and the vertical planes [29–31]. FP is measured as:

$$P = \frac{I_{||} - GI_{+}}{I_{||} + GI_{+}} \tag{1}$$

where P is the polarization ratio, and $I_{||}$ and I_{+} are the parallel and perpendicular fluorescence intensity (FI) to the exciting light, respectively. G is an instrument and wavelength dependent correction factor to compensate for the polarization bias of the detection system.

FLIM experiments used a DCS-120 Confocal Scanning FLIM System based on TCSPC module (SPC-150, Becker & Hickl, Berlin, Germany) that works in reversed start-stop configuration, and an OLYMPUS IX-81 microscope with a 10x, NA = 0.4 objective [32]. The excitation source was a 470 nm Laser diode (Becker & Hickl, BDL-470-SMC) with a repetition frequency of 50 MHz and 5 mWatt power. The data analysis software (SPCImage, Becker & Hickl GmbH) allowed curve fitting of the acquired data on a pixel-by-pixel basis using a weighted least-squares numerical approach, and estimated the instrument response function (IRF) from the fluorescence signal itself [33].

The FLIM data can be considered as an array of pixels, each containing a large number of time channels spread over the fluorescence decay. To obtain a 'FLT image' from this data, a fit procedure was performed in all the pixels of the image. For FLT measurements of fluorophores molecules conjugated to GNPs, a double exponential model was chosen:

$$f(t) = a_1\, e^{-t/\tau_1} + a_2\, e^{-t/\tau_2} \tag{2}$$

where $f(t)$ is the fluorescence decay function, a_1 and a_2 are the amplitudes, and τ_1 and τ_2 are the FLT of the exponentials components, respectively. In our re-

Table 1 Zeta-potential and DLS for different GNPs. Each value represents mean ± STD (n = 3).

Characteristic parameter	Zeta-potential [mV]	DLS [d. nm]
Free GNP	–43.3 ± 2.9	26 ± 0.6
PEG-GNP	–29.7 ± 3.1	46 ± 1.5
LY-GNP	–27.0 ± 2.2	67 ± 1.4
FreeLY-GNP-LY-Mix	–31.7 ± 0.5	64 ± 3

search τ_1 is chosen to be fixed to the value of FLT of the free fluorophore, as measured and fitted by using a single exponential model for FLT decay (see *Fluorescence lifetime method* in the results section). τ_2 is the unconstrained FLT component, representing the effect of the conjugation on the FLT, indicating the level of conjugation.

3. Results and discussion

We examined the binding of LY dye to GNPs with traditional methods for characterization of changes in size, surface potential and absorption spectra. We compared the traditional methods to the new fluorescence-based methods for characterizing changes in emission spectra, steady state FP and FLT. The GNPs, PEG-GNPs and LY-GNPs were characterized after each coating step.

3.1 Basic NPs characterization

Zeta potential values for the successive steps of the synthesis of LY-GNP are shown in Table 1. While free GNPs had zeta potential of –43.3 ± 2.9 mV, the other NPs had zeta potential of –29.7 ± 3.1, –27.0 ± 2.2 and –31.7 ± 0.5 mV for PEG-GNPs, LY-GNPs and NPs in FreeLY-GNP-LY-Mix respectively. For DLS measurements, Free GNP and PEG-GNP had hydrodynamic diameters of 26 ± 0.6 and 46 ± 1.5 nm respectively. LY-GNP and NPs in FreeLY-GNP-LY-Mix had higher hydrodynamic diameters (67 ± 1.4 nm and 64 ± 3 nm respectively). Both zeta potential and DLS measurements enable the differentiation between the free GNPs and the PEG coated GNPs. Additional coatings have not led to conclusive outcome. These results highlight the difficulty in using these methods for differentiation between the sub-products of NPs conjugated to molecules along the synthesis.

Steady-state absorption spectra (Figure 2A) exhibited broad bands. The LY-free was well distinguished with maximum at 429 nm (Table 2), which is in agreement with literature values for H_2O solvent [34]. The GNPs spectra were more adjacent, and displayed that the free GNP and PEG-GNP were approximately undistinguishable with maxima at 523 nm and 524 nm respectively, and the LY-GNP and NPs in FreeLY-GNP-LY-Mix were more separated and broader with maxima at 527 nm for both. The red shift and broadening of the spectra are well known phenomena resulted when organic layer coating increases energy absorption from irradiated light. Meaning, the red shift phenomenon is not due to molecular changes in the LY characteristics but due to the conjugation to the GNP. These results are in agreement with the zeta potential finding and the increase size of the NPs from the DLS measurements.

Steady-state fluorescence spectra (Figure 2B) demonstrated excited dynamic only for free LY, LY-

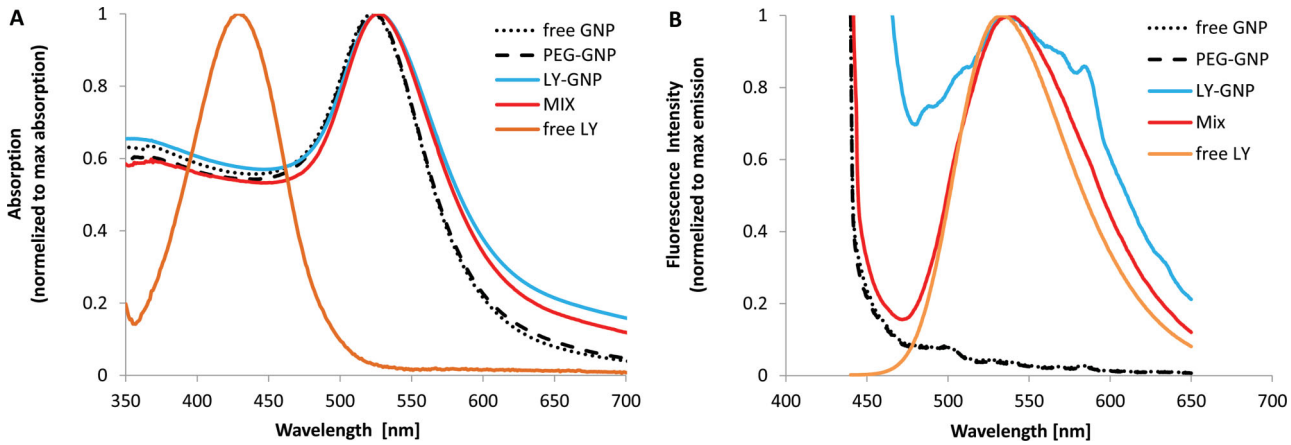

Figure 2 Normalized steady-state absorption and fluorescence spectra for different GNPs. (**A**) Absorption curves for Free-GNP (dots black), PEG-GNP (dash black), LY-GNP (solid blue), FreeLY-GNP-LY-Mix (solid red, marked as 'Mix'), and free LY (solid orange). Each sample of absorption curve was normalized according to its peak. (**B**) Fluorescence spectra for each NP mentioned in A. Lower peak for GNPs, PEG-GNP and LY-GNP indicates reflectance of excitation light from GNP and not a fluorescent signal. Curves of LY-GNP, Mix and free LY were normalized according to their peaks in the range [470–650] nm.

Table 2 Absorption and emission maxima wave length for different GNPs. The peaks are in alignment with normalized absorption and fluorescence spectra in Fig. 2. MIX stands for FreeLY-GNP-LY-Mix sample.

	Free GNP	PEG-GNP	LY-GNP	MIX	Free LY
Absorption max [nm]	523	524	527	527	429
Emission max [nm]	–	–	536.5	538.5	533.5

GNP and FreeLY-GNP-LY-Mix NPs, with maxima at 533.5, 536.5, and 538.5 nm, respectively (Table 2) (excitation wavelength at 430 nm). These results are in agreement with the literature values of 530 nm for LY in H_2O solvent [34]. Curves were normalized according to the peaks of each excited spectrum in the range 470–650 nm. LY-GNP displayed broader spectrum in comparison to the other NPs. Its' noisier signal was probably due to lower FI (data not shown) following spectroscopic parameters as described at *Fluorescence lifetime Method* section below. As expected, Free GNP and PEG-GNP showed an exponential decay spectrum, which suggests that they had no excitation features. The spectra analysis demonstrates again the difficulty in differentiating between GNP coated with LY and a FreeLY-GNP-LY-Mix NPs. The difficulty is much clearer for absorption, while for excitation the broadening spectrum of LY-GNP is more distinguishing.

3.2 New approach for GNPs-LY conjugation analysis

Fluorescence polarization method

FP measurements of GNPs with LY coating are shown in Figure 3. When the rotation correlation time of the fluorophore is much shorter compared to the FLT, the excited fluorophore quickly changes orientation upon emission, resulting in low steady-state FP values [24, 29, 35]. This is typical for small molecules. Indeed, the FP for free LY was 0.02 ± 0.01 (number of repetitions (n) = 9). However, when the rotation time is much longer compared to FLT, the excited fluorophore hardly changes orientation upon emission, and results in high polarization values [29]. This is typical for large molecules structure. In this case the structure was caused by the binding of the LY dye to GNPs, with FP of 0.12 ± 0.03 (n = 9, t-test $p = 1.6e^{-6}$ vs. LY). It is expected that for the Free-LY-GNP-LY-Mix sample, the combined free and binding fluorophores, will result in intermediate PF values, which indeed were 0.04 ± 0.01 (n = 9, $p = 5.73e^{-5}$ vs. LY, and $p = 1.9e^{-6}$ vs. LY-GNP). The

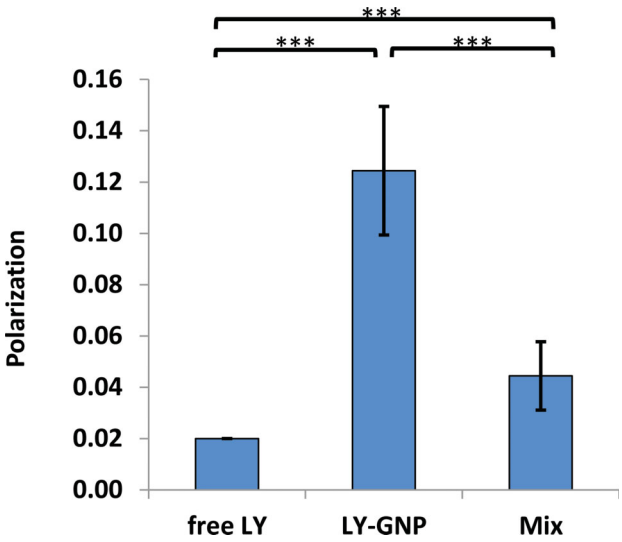

Figure 3 Fluorescence polarization for the different NPs. Data are presented as mean ± STD (n = 9), where the samples excitation wavelength was 430 nm, and emission wavelengths were organized in 3 group of 3 for 540, 550, and 560 nm, without any significant change for sub-groups. Only intensity > 20 was taken for analysis. Significance levels (t-test) are indicated in the figure (*$p < 0.05$).

desired product LY-GNP showed significantly higher polarization than the other sub-products, indicating on the strength of FP for dyes conjugation analysis.

Fluorescence lifetime method

FLIM was used to measure the average FLT of LY dye coating of GNPs core [36, 37]. Placing a fluorophore in the vicinity of a metal nanoparticle with surface plasmon resonances (like gold and silver) creates coupling between the oscillating electron systems and the NP plasmon resonances [6, 38]. Theoretical and experimental studies have demonstrated changes in fluorescence quenching, excitation and FLT when the distance between the metal NP and the fluorophore were on the scale of 1–100 nm [39, 40]. Imaging of time domain fluorescence of free LY, LY-GNP and FreeLY-GNP-LY-Mix NPs are presented (Fig. 4A), where the array of pixels represent a fluorescence time decay instead of FI. The decay was modeled with a double exponential, where the 1st FLT term was fixed to the FLT of free LY (5.37 ± 0.03 ns, (n = 6)) measured and fitted using a single exponential, and in agreement with literature values of 5.7 ns [34]. The 2nd FLT term (τ_2, see Eq. (2)) was unconstrained. τ_2 represents FLT alterations as a result of the conjugation of the fluorophore LY and the GNPs. The measured and fitted τ_2 term for free LY, LY-GNP and FreeLY-GNP-LY-Mix NPs is shown in normalized histograms (Figure 4B), showing a much broader distribution for LY-GNPs and a shift

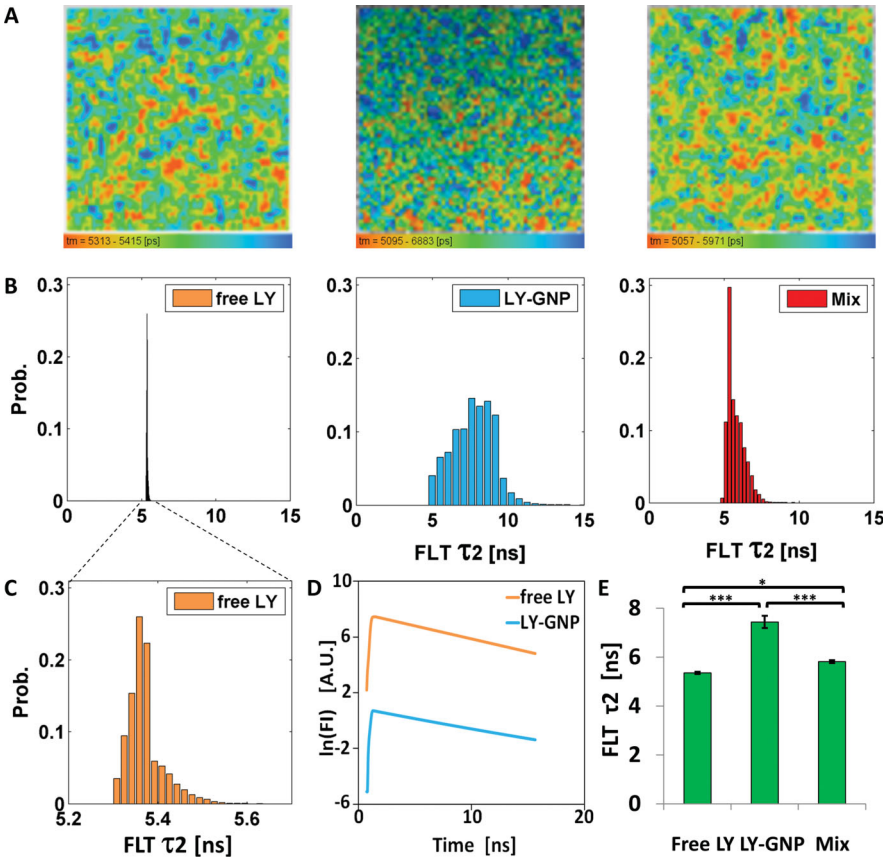

Figure 4 Fluorescence lifetime. (**A**) Florescence lifetime color coded imaging (FLIM) showing as an array of pixels, each represent a FI time decay. A color coded FLT sacle is presented bellow each image, where shorter FLT marked in red and longer in blue. FLT for free LY (left, range of 5.3–5.4 ps), LY-GNP (middle, range of 5.0–6.9 ps) and FreeLY-GNP-LY-Mix (right, range of 5.0–6.0 ps). (**B**) Histogram of the τ_2 lifetime for each of the FLIM in A, where τ_1 lifetime was fixed to the FLT of free LY. Normalized by the sum of events. (**C**) Enlargement of LY free histogram from B. (**D**) FLIM intensity decay curves for free LY and LY-GNP (**E**) Mean ± STD τ_2 lifetime for the different NPs (free LY n = 4), LY-GNP n = 6, and Mix n = 2). Significance levels (t-test) are indicated in the figure (*$p < 0.05$). LY FLT for H_2O solvent is 5.7 ns [34].

of the mean τ_2 to a higher values. The broadening of the FLT distribution for LY-GNPs is also due to the lower FI in this sample. Average FLT τ_2 for free LY was 5.35 ± 0.04 ns (n = 4) (Figure 4C, E), which is expected when there are no constraints on the fluorophores, so the FLT is similar to the one with single exponential model. The LY-GNP τ_2 term was 7.44 ± 0.25 ns (n = 6, p = 7.2e^{-7} vs. free LY), while the FreeLY-GNP-LY-Mix NP τ_2 term was 5.81 ± 0.05 ns (n = 2, p = 0.015 vs. free LY, and p = 3e^{-6} vs. LY-GNP). The FLT of LY-GNP was increased in comparison to free LY, probably as a result of large distance between the dye and the GNPs surface, which was created when using large PEG as an intermediate layer connecting the metal NP and the fluorophore.

The increased FLT may be also the outcome of the linkage to the GNP, that is larger than the fluorescent molecule [35].

Table 2 contains the FLT decay fitted with the double exponential model. The weight of term τ_2 is a_2, χ^2 is the root mean squares of the fitted model, and #Photons is the number of photons read in the detector. The 3 fluorophore samples (LY-GNP, MIX and Free LY) showed a χ^2 values closed to 1, indicating good data fitting results [32]. The number of photons for the free LY (14005 ± 2015, (n = 4)) is much higher compared to the LY-GNP (with 48 ± 20, n = 6), and the FreeLY-GNP-LY-Mix (with 220 ± 4, n = 2). However, these results are expected as the GNPs decrease the quantum yield [18] of the LY due to the overlap in their quantum levels. In order to keep the FLIM system with similar conditions, as required [32], for all samples, the optical properties were identical including the excitation laser power (5 mWatt as described at 2.2 above).

Table 3 Fluorescence lifetime parameters. The NPs are identical to those in Fig. 4. Parameters being presented: a_2 is the weight of FLT τ_2 in a double exponential model of FLT decay (see Eq. (2)), χ^2 is the root mean squares of the model fitting, and #Photons is the number of photons read in the detector. Data are represented as mean ± STD (free LY n = 4, LY-GNP n = 6, and Mix n = 2)

	Free LY	LY-GNP	MIX
FLT τ_2 [ns]	5.35 ± 0.04	7.44 ± 0.25	5.81 ± 0.05
a_2	81% ± 0.10	46% ± 0.09	56% ± 0.05
χ^2	2.30 ± 0.69	1.32 ± 0.14	1.08 ± 0.01
#Photons	14005 ± 2015	48 ± 20	220 ± 4

4. Conclusion

Measuring the decay FLT and steady state FP provides insights into the evaluation methods of binding fluorophores to other molecules. We have demonstrated a new fluorescence-based approach, useful to characterize and analyze the binding of GNPs with LY surface coating. Using the traditional spectrum analysis methods, DLS, zeta potential and emission spectrum, has led to difficulties in differentiating between LY-GNP (the conjugated complex) and a mixture of coated NP and free dyes. Our new approach combining FP and FLT measurements has led to a reliable separation and evaluation of conjugation rate. To note, a successful assessment of the conjugation was achieved independently using the two new fluorescence-based methods, showing a significant increase in FP and FLT for the LY-GNP samples. However, combining the two methods present a clear-cut determination of the surface conjugation process outcome. We propose the new procedure as a general reliable method for evaluating the quality of conjugation of nanocomposites to fluorescent tagging. We encourage the use of the approach when investigating new nanocomposites materials incorporated in cells. Specifically, for neuroscientists the study of LY-GNP nanocomposites is important for the development of novel imaging and therapeutic nano-based tools.

Acknowledgements Special thanks for the help given by Tsviya Nayhoz from Faculty of Engineering Bar-Ilan University, and Zehavit Eizig from Biophysical Schottenstein Center, Physics Department Bar-Ilan University. This work was partially supported by the Research and Development – Chief Scientist Nofar grant, ISF grant (#927432) and by the ICRF grant (R.P.).

Author biographies Please see Supporting Information online.

References

[1] E. C. Dreaden, A. M. Alkilany, X. Huang, C. J. Murphy, and M. A. El-Sayed, Chem. Soc. Rev **41**, 7 (2012).
[2] S. Jain, D. G. Hirst, and J. M. O'Sullivan, Br. J. Radiol. **85**, 1010 (2012).
[3] M. Shilo, T. Reuveni, M. Motiei, and R. Popovtzer, Nanomedicine (Lond). **7**, 2 (2012).
[4] C. Sun, J. S. H. Lee, and M. Zhang, Adv. Drug Deliv. Rev. **60**, 11 (2008).
[5] M. J. Ruedas-Rama, J. D. Walters, A. Orte, and E. A. H. Hall, Anal. Chim. Acta **751**, 1 (2012).
[6] A. P. Demchenko, Methods Appl. Fluoresc. **1**, 2 (2013).
[7] B. Hötzer, I. L. Medintz, and N. Hildebrandt, Small **8**, 15 (2012).
[8] D. Fixler and Z. Zalevsky, Nano Lett. **13**, 12 (2013).
[9] R. Ankri, D. Leshem-Lev, D. Fixler, R. Popovtzer, M. Motiei, R. Kornowski, E. Hochhauser, and E. I. Lev, Nano Lett. **14**, 5 (2014).
[10] W. H. De Jong and P. J. A. Borm, Int. J. Nanomedicine **3**, 2 (2008).
[11] M. Ferrari, Nat. Rev. Cancer **5**, 3 (2005).
[12] N. a. Kotov, J. O. Winter, I. P. Clements, E. Jan, B. P. Timko, S. Campidelli, S. Pathak, A. Mazzatenta, C. M. Lieber, M. Prato, R. V. Bellamkonda, G. a. Silva, N. W. S. Kam, F. Patolsky, and L. Ballerini, Adv. Mater. **21**, 40 (2009).
[13] D. Son, J. Lee, S. Qiao, R. Ghaffari, J. Kim, J. E. Lee, C. Song, S. J. Kim, D. J. Lee, S. W. Jun, S. Yang, M. Park, J. Shin, K. Do, M. Lee, K. Kang, C. S. Hwang, N. Lu, T. Hyeon, and D.-H. Kim, Nat. Nanotechnol. **9**, 5 (2014).
[14] P. Polak, Z. Zalevsky, and O. Shefi, Int. J. Biol. Macromol. **59**, 134 (2013).
[15] J. R. Lakowicz, Plasmonics **1**, 1 (2006).
[16] T. Ming, H. Chen, R. Jiang, Q. Li, and J. Wang, J. Phys. Chem. Lett. **3**, 2 (2012).
[17] H. Y. Lee, H. Son, J. M. Lim, J. Oh, D. Kang, W. S. Han, and J. H. Jung, Analyst **135**, 8 (2010).
[18] D. Fixler, T. Nayhoz, and K. Ray, ACS Photonics **1**, 9 (2014).
[19] J. M. Bergen, H. A. von Recum, T. T. Goodman, A. P. Massey, and S. H. Pun, Macromol. Biosci. **6**, 7 (2006).
[20] M. Shilo, M. Motiei, P. Hana, and R. Popovtzer, Nanoscale **6**, 4 (2014).
[21] A. Verma and F. Stellacci, Small **6**, 1 (2010).
[22] G. a Silva, Nat. Rev. Neurosci. **7**, 1 (2006).
[23] C. M. Lamy, O. Sallin, C. Loussert, and J.-Y. Chatton, ACS Nano **6**, 2 (2012).
[24] J. R. Lakowicz, Principles of Fluorescence Spectroscopy, Springer, 2006 [Online]. Available: http://www.springer.com/chemistry/analytical+chemistry/book/978-0-387-31278-1 [Accessed: 30-Jun-2014].
[25] K. Saha, S. S. Agasti, C. Kim, X. Li, and V. M. Rotello, Chem. Rev. **112**, 5 (2012).
[26] R. Ankri, H. Duadi, M. Motiei, and D. Fixler, J. Biophotonics **5**(3), 263–273 (2012).
[27] M. Hanani, J. Cell. Mol. Med. **16**, 1 (2012).
[28] B. Y. B. V. Enustun, Coagulation of Colloidal Gold **730**, 18 (1963).
[29] Invitrogen, Fluorescence Polarization Technical Resource Guide (2006).
[30] D. Fixler, R. Tirosh, N. Zurgil, and M. Deutsch, J. Biomed. Opt. **10**, 3 (2005).
[31] D. Fixler, R. Tirosh, T. Zinman, A. Shainberg, and M. Deutsch, Biochem. Biophys. Res. Commun. **300**, 1 (2003).
[32] L. Turgeman and D. Fixler, IEEE Trans. Biomed. Eng. **60**, 6 (2013).
[33] Becker & Hickl GmbH, DCS-120 Confocal Scanning FLIM Systems, user handbook, no. April, 2012.
[34] A. Fürstenberg and E. Vauthey, Photochem. Photobiol. Sci. **4**, 3 (2005).

[35] D. Fixler, Y. Namer, Y. Yishay, and M. Deutsch, IEEE Trans. Biomed. Eng. **53**, 6 (2006).
[36] F. E. Hernández, S. Yu, M. García, and A. D. Campiglia, J. Phys. Chem. B **109**, 19 (2005).
[37] Y. Fu, J. Zhang, and J. R. Lakowicz, J. Am. Chem. Soc. **132**, 16 (2010).
[38] E. Fort and S. Grésillon, J. Phys. D. Appl. Phys. **41**, 1 (2008).
[39] J. Malicka, I. Gryczynski, Z. Gryczynski, and J. R. Lakowicz, Anal. Biochem. **315**, 1 (2003).
[40] P. Anger, P. Bharadwaj, and L. Novotny, Phys. Rev. Lett. **96**, 11 (2006).